Theory of Two-Phase Detonation—Part II: Structure

J. M. POWERS,

Department of Aerospace and Mechanical Engineering, University of Notre Dame, Notre Dame, Indiana 46556

D. S. STEWART, and H. KRIER

University of Illinois at Urbana-Champaign, Urbana, Illinois 61801

The structure of a two-phase steady detonation in a granulated solid propellant is studied, and existence conditions for a one-dimensional, steady two-phase detonation are given. Ordinary differential equations from continuum mixture theory are solved numerically to determine steady wave structure. In the limiting case where heat transfer and compaction effects are negligible, the model reduces to two ordinary differential equations that have a clear geometrical interpretation in a two-dimensional phase plane. This two-equation model predicts results that are quite similar to those of the full model. This suggests that in the limited parameter space studied heat transfer and compaction are not important mechanisms in determining the detonation structure. It is found that strong and Chapman–Jouguet (CJ) detonation solutions with a leading gas phase shock and unshocked solid can be admitted, as can weak and CJ solutions with an unshocked gas and solid. As for one-phase materials, the CJ wave speed is the speed of propagation predicted for an unsupported, one-dimensional, two-phase detonation. It is predicted that there is no admissible CJ structure with a single leading gas phase shock and unshocked solid below a critical value of initial bulk density. This result cannot be predicted from equilibrium end state analysis. Thus it is concluded that it is essential to consider reaction zone structure when assessing potential solutions.

NOMENCLATURE

A	function of solid phase variables
A_{ij}	matrix function of solid phase variables
B	function of solid phase variables
B_i	vector of solid phase variables
c_v	specific heat at constant volume
C	function of solid phase variables
D	steady wave speed or function of solid phase variables
e	internal energy
E	function of solid phase variables
f	function of solid density and volume fraction
F	function of solid phase variables
g	function of solid density and volume fraction
h	heat transfer constant or function of solid density and volume fraction
i	subscript, $i = 1$, gas; $i = 2$, solid
ig	ignition
K	shock constant
L	length scale
m	burning exponent
M	Mach number
P	pressure
q	chemical energy
r	particle radius
R	gas constant
T	temperature
u_j	vector of solid phase variables
v	velocity in wave frame
z	progress variable

Greek Symbols

α	burning constant
β	drag constant
γ	Gruneisen coefficient $+1$
μ_c	compaction viscosity

0010-2180/90/$3.50

ξ distance in wave frame
π dimensionless parameter
ρ density
σ non-ideal solid parameter
ϕ volume fraction
ω sound speed

INTRODUCTION

Deflagration-to-detonation transition (DDT) in granular solid propellants is an important unsolved problem. Experiments by Griffiths and Groocock [1] and Bernecker and Price [2, 3] have demonstrated the transition to detonation in granular HMX. Many researchers have modeled the DDT process using one-dimensional two-phase reactive flow models. The work of Butler et al. [4] showed for the first time in the archival open literature that a two-phase model could predict a transition from a deflagration to a steady detonation. Since then many models have been presented that describe the transient processes that can ultimately lead to a steady detonation in a two-phase mixture. Among these models are those of Butler and Krier [5], Baer and Nunziato [6], Baer et al. [7], Akhatov and Vainshtein [8], and Markatos [9].

Although unsteady two-phase flow equations have been used extensively to model DDT, the more fundamental problem of two-phase steady detonation has largely been ignored. In the field of solid propellant combustion, only the work of Krier and Mozafarrian [10] considers steady detonation solutions to the two-phase reactive flow equations. This work is of limited value because of the assumption of an incompressible solid phase. In addition there is question as to whether the unsteady form of the model equations of this work are hyperbolic [11]. Multiphase steady detonation theory has been studied by Sharon and Bankoff [12] and Condiff [13] as it applies to vapor explosions in mixtures of hot liquid metals and water. Large differences in the assumptions and constitutive theory prevent a direct application of this theory to the problem of steady detonation in granulated propellants.

There are many reasons to study steady two-phase detonation theory. As opposed to unsteady DDT theory, which considers solutions to time-dependent partial differential equations, the steady two-phase detonation is described by the solution of ordinary differential equations. This allows the use of the powerful technique of phase space analysis to describe the solutions. In addition with the steady equations, it is not necessary to use special numerical techniques to describe shock discontinuities. Instead the shock state is specified by an exact solution to algebraic shock discontinuity equations. Predictions of steady theory can be compared to predictions of steady detonations by unsteady models as an additional means of verification of those models. In addition knowledge of the steady solution is necessary for stability or multidimensional studies.

There are several shortcomings to current two-phase detonation theory. First and foremost, there is no clear link between two-phase detonation theory and one-phase CJ and ZND detonation theory. As described by Fickett and Davis [14], one-phase CJ theory identifies three classes of detonation end states that depend on the velocity of a supporting piston: a weak, strong, and CJ end state. Because the gas velocity relative to the wave head is sonic at the CJ end state, the CJ wave can propagate without disturbance from trailing rarefactions and thus is a potential equilibrium end state for an unsupported detonation. The strong end state is subsonic and thus requires piston support to maintain a steady speed. The weak end state is supersonic and thus not ruled out by CJ theory. ZND theory describes the structure that links the ambient state to the equilibrium end state described by CJ theory. In its simplest form, one ordinary differential equation is integrated to describe the reaction zone structure. The structure consists of an inert shock discontinuity that initiates the reaction followed by a zone where the reaction goes to completion. ZND theory rules out the weak state for a detonation with a simple one-step irreversible reaction with a leading shock. ZND theory identifies a structure linking the shocked state to both the strong and CJ end states. As most two-phase detonation studies have concentrated on transient events, there has been little discussion describing two-phase detonations in the context of this established one-phase theory.

There are other more specific deficiencies in

current two-phase theory. First, current two-phase detonation theory does not identify the role or necessity of either shock jumps or sonic points in the detonation structure. The role of both is clearly identified in the one-phase theory. Next, in most two-phase detonation studies, the equilibrium end states are not identified. Powers et al. [15] have studied the complete reaction gas phase end state and identified two-phase equivalents to the CJ, strong, and weak solutions. To find these equivalents, it was necessary to assume that the complete reaction state was an equilibrium end state. This assumption is questioned because the model equations for two-phase granular materials are singular at the complete reaction state. The singularity arises because the forcing functions in the governing equations are inversely proportional to the particle radius, which approaches zero near complete reaction. The effects of this singularity have not previously been examined. Finally, steady two-phase detonation structures predicted by unsteady models do not contain enough resolution to distinguish details of the structure. In Refs. 5 and 6, it appears that the steady detonation reaction zone structure is defined over a small number of finite difference cells. As the shock wave is also spread through these cells, it is difficult to distinguish the shock from the reaction zone.

This article focuses on a comparison of two-phase detonation theory to one-phase detonation theory, the technique and peculiarities of two-phase steady state modeling, a detailed example of a steady-state two-phase detonation structure, and an example of a nonphysical structure. The description of the steady-state modeling technique can be applied to general two-phase systems and should not be thought of as only valid for detonation systems. The model is an improvement of the models of Butler and Krier [5] and Baer and Nunziato [6]. It was first presented in Ref. 15 and studied in more detail in Ref. 16, which accompanies this article. The model is presented in both steady dimensional and dimensionless form. It will then be reduced to four ordinary differential equations in four unknowns. Next a technique is described for studying the singularity at complete reaction and an additional singularity that arises when the solid velocity is sonic. For completeness, shock waves in two-phase systems and complete reaction equilibrium end states are briefly discussed. It is then shown how in special limits the four ordinary differential equations reduce to two ordinary differential equations. An analysis of these equations in the phase plane is provided. This analysis clearly identifies both the gas and solid phase end states. The two- and four-equation models are then used to predict two-phase analogs to CJ, strong, and weak detonation structures. Finally it is shown how this model can predict a nonphysical solution.

STEADY-STATE MODEL

For this article the nomenclature and equations of Refs. 15 and 16 are adopted. The steady form of the two-phase model equations of Refs. 15 and 16 is found by transforming the equations to the steady wave frame using the transformation $\xi = x - Dt$, $v_i = u_i - D$ and assuming in this frame that all time derivatives are zero. Here D is the steady wave speed, v is the relative velocity, and ξ the distance in the steady wave frame. The gas and solid mass equations in conservative form are, respectively,

$$\frac{d}{d\xi}(\rho_1\phi_1 v_1) = \left(\frac{3}{r}\right)\rho_2\phi_2\alpha P_1{}^m H(T_2 - T_{ig}), \quad (1)$$

$$\frac{d}{d\xi}(\rho_2\phi_2 v_2) = -\left(\frac{3}{r}\right)\rho_2\phi_2\alpha P_1{}^m H(T_2 - T_{ig}). \quad (2)$$

The gas and solid momentum equations in conservative form are, respectively,

$$\frac{d}{d\xi}(\rho_1\phi_1 v_1{}^2 + P_1\phi_1) = \left(\frac{3}{r}\right)\rho_2\phi_2\alpha P_1{}^m v_2 H(T_2 - T_{ig}) + \beta\frac{\phi_1\phi_2}{r}(v_2 - v_1), \quad (3)$$

$$\frac{d}{d\xi}(\rho_2\phi_2 v_2{}^2 + P_2\phi_2) = -\left(\frac{3}{r}\right)\rho_2\phi_2\alpha P_1{}^m v_2 H(T_2 - T_{ig}) - \beta\frac{\phi_1\phi_2}{r}(v_2 - v_1). \quad (4)$$

The gas and solid energy equations in conservative form are, respectively,

$$\frac{d}{d\xi}[\rho_1\phi_1 v_1(e_1 + v_1^2/2 + P_1/\rho_1)] = \left(\frac{3}{r}\right)\rho_2\phi_2\alpha P_1^m H(T_2 - T_{ig})(e_2 + v_2^2/2) + \beta\frac{\phi_1\phi_2}{r}(v_2 - v_1) + h\frac{\phi_1\phi_2}{r^{1/3}}(T_2 - T_1), \tag{5}$$

$$\frac{d}{d\xi}[\rho_2\phi_2 v_2(e_2 + v_2^2/2 + P_2/\rho_2)] = -\left(\frac{3}{r}\right)\rho_2\phi_2\alpha P_1^m H(T_2 - T_{ig})(e_2 + v_2^2/2) - \beta\frac{\phi_1\phi_2}{r}(v_2 - v_1) - h\frac{\phi_1\phi_2}{r^{1/3}}(T_2 - T_1). \tag{6}$$

The compaction equation is given by

$$v_2\frac{d\phi_2}{d\xi} = \frac{\phi_1\phi_2}{\mu_c}\left(P_2 - P_1 - \frac{P_{20} - P_{10}}{\phi_{20}}\phi_2\right) - \left(\frac{3}{r}\right)\phi_2\alpha P_1^m H(T_2 - T_{ig}). \tag{7}$$

Number conservation is expressed as

$$\frac{d}{d\xi}\left(\frac{\phi_2 v_2}{r^3}\right) = 0. \tag{8}$$

The gas phase is described by a virial state equation. Expressions for the thermal and caloric state equations and frozen sound speed are

$$P_1 = \rho_1 R T_1(1 + b\rho_1), \tag{9}$$

$$e_1 = c_{v1}T_1, \tag{10}$$

$$\omega_1^2 = RT_1[1 + 2b\rho_1 + (R/c_{v1})(1 + b\rho_1)^2]. \tag{11}$$

The solid phase is described by a Tait equation of state. The thermal and caloric state equations and frozen sound speed are given by

$$P_2 = (\gamma_2 - 1)c_{v2}\rho_2 T_2 - \frac{\rho_{20}\sigma}{\gamma_2}, \tag{12}$$

$$e_2 = c_{v2}T_2 + \frac{\rho_{20}\sigma}{\gamma_2\rho_2} + q, \tag{13}$$

$$\omega_2^2 = \gamma_2(\gamma_2 - 1)c_{v2}T_2. \tag{14}$$

The mixture is constrained to be saturated so that

$$\phi_1 + \phi_2 = 1. \tag{15}$$

For the eight ordinary differential equations eight initial conditions are chosen. At $\xi = 0$ it is required that

$$\rho_1 = \rho_{10}, \quad \rho_2 = \rho_{20}, \quad T_1 = T_0, \quad T_2 = T_0, \quad \phi_1 = \phi_{10}, \quad r = r_0, \quad v_1 = -D, \quad v_2 = -D. \tag{16}$$

By substituting the initial equations into the differential Eqs. 1–8, it is seen that the ambient state is an equilibrium state, that is, all forcing functions are identically zero at the ambient state.

Though this model has been developed to describe general reactive granular materials, the granular explosive HMX will be studied here. Numerical values for the parameters for HMX are listed in Table 1. When available, references are

TABLE 1

Dimensional Input Parameters

Parameter	Reference	Unit	Value
a	[5]	[m/(s Pa)]	2.90×10^{-9}
ρ_{10}		[kg/m^3]	1.00×10^{1}
m	[5]		1.00×10^{0}
β		[kg/(s m^2)]	1.00×10^{4}
ρ_{20}	[5, 6]	[kg/m^3]	1.90×10^{3}
h		[J/(s K m$^{8/3}$)]	1.00×10^{7}
c_{v1}	[6]	[J/(kg K)]	2.40×10^{3}
c_{v2}	[5, 6]	[J/(kg K)]	1.50×10^{3}
R		[J/(kg K)]	8.50×10^{2}
σ	[21]	[(m/s)^2]	8.98×10^{6}
q	[5]	[J/kg]	5.84×10^{6}
r_0	[5, 6]	[m]	1.00×10^{-4}
b		[m^3/kg]	1.10×10^{-3}
γ_3	[21]		5.00×10^{0}
μ_c		[kg/(m s)]	1.00×10^{6}
T_0		[K]	3.00×10^{2}
T_{ig}		[K]	$3.00 \times 10^{2}+$

listed in Table 1 for each of the parameters. Other parameters have been estimated for this study. Some parameter values were estimated so that a steady two-phase detonation structure could be predicted. The initial gas density, gas temperature, and ignition temperature have been arbitrarily chosen to be 10 kg/m^3, 300 K, and 300+ K, respectively. The ignition temperature was chosen to be the ambient temperature because it represents a bulk solid temperature. For the flow of a shocked gas past particles, there will be an energy transfer to the solid that could cause the local solid surface temperature to reach ignition level. At the same time the majority of the solid remains at the ambient temperature. Thus it was hypothesized that reaction could begin when the bulk solid temperature was arbitrarily near the ambient temperature. Drag and heat transfer parameters roughly match empirical formulae given in Ref. 17. Comparisons of the drag and heat transfer models can be found in Ref. 11. The gas constant R and virial coefficient b have been chosen such that predictions of CJ detonation states match the CJ detonation states predicted by the thermochemistry code TIGER [18] as reported in Ref. 5. Detailed comparisons are found in Ref. 15. The solid parameters σ and γ_2 have been chosen such that solid shock and compaction wave predictions match experimental shock [19] and compaction wave data [20]. These comparisons are described in Ref. 21. As reported by Baer and Nunziato [6], there are no good estimates for the compaction viscosity μ_c. In Ref. 6, a value for compaction viscosity of 10^3 kg m^{-1}s^{-1} was chosen. To demonstrate the existence of a two-phase detonation, it was necessary to choose a higher value, 10^6 kg m^{-1} s^{-1}, for the compaction viscosity.

The model equations are written next in dimensionless form, where an asterisk indicates a dimensionless quantity:

$$\xi_* = \xi/L, \quad v_{*i} = v_i/D, \quad P_{*i} = P_i/(\rho_{i0}D^2),$$

$$\rho_{*i} = \rho_i/\rho_{i0}, \quad e_{*i} = e_i/D^2,$$

$$T_{*i} = c_{vi}T_i/D^2, \quad r_* = r/L, \quad i = 1, 2.$$

Here L is a length scale which can be associated with the reaction zone length. The following independent dimensionless parameters are defined:

$$\pi_1 = 3\alpha\rho_{10}{}^m D^{2m-1}, \quad \pi_2 = \beta/(\rho_{20}D),$$

$$\pi_3 = hL^{2/3}/(\rho_{20}c_{v1}D), \quad \pi_4 = m,$$

$$\pi_5 = \rho_{10}/\rho_{20}, \quad \pi_6 = c_{v1}/c_{v2},$$

$$\pi_7 = R/c_{v1} + 1, \quad \pi_8 = \sigma/(\gamma_2 D^2),$$

$$\pi_9 = \rho_{20}DL/\mu_c, \quad \pi_{10} = q/D^2,$$

$$\pi_{11} = \phi_{10}, \quad \pi_{12} = r_0/L,$$

$$\pi_{13} = b\rho_{10}, \quad \pi_{14} = c_{v2}T_0/D^2, \quad \pi_{17} = \gamma_2.$$

The following dependent dimensionless parameters are defined:

$$\pi_{18} = \pi_{11} + \frac{1 - \pi_{11}}{\pi_5},$$

$$\pi_{19} = (\pi_7 - 1)\pi_6\pi_{14}(1 + \pi_{13}),$$

$$\pi_{20} = 1 - \pi_{11},$$

$$\pi_{21} = (\pi_{17} - 1)\pi_{14} - \pi_8,$$

$$\pi_{22} = \pi_{11}\left[\pi_6\pi_{14} + \frac{1}{2} + \pi_{19}\right] + \frac{1 - \pi_{11}}{\pi_5}\left[\pi_{14} + \pi_{10} + \frac{1}{2} + \pi_{21}\right],$$

$$\pi_{23} = \pi_{11}\pi_{19} + \frac{1 - \pi_{11}}{\pi_5}\pi_{21},$$

$$\pi_{15} = \frac{\pi_{21} - \pi_5\pi_{19}}{1 - \pi_{11}}.$$

The dimensionless solid phase mass, momentum, and energy equations written in nonconservative form are given below (for compact notation, the asterisks are dropped, and it is understood that unless otherwise indicated, all variables are

dimensionless):

$$\frac{d}{d\xi}[\rho_2\phi_2 v_2] = -\pi_1 \frac{\rho_2\phi_2 P_1^{\pi_4}}{r}, \tag{17}$$

$$\rho_2\phi_2 v_2 \frac{dv_2}{d\xi} + \frac{d}{d\xi}[P_2\phi_2] = -\pi_2[v_2 - v_1]\frac{\phi_1\phi_2}{r}, \tag{18}$$

$$\rho_2 v_2 \frac{de_2}{d\xi} + P_2 \frac{dv_2}{d\xi} = -\pi_3[\pi_6 T_2 - T_1]\frac{\phi_1}{r^{1/3}}. \tag{19}$$

The dimensionless compaction equation is

$$v_2 \frac{d\phi_2}{d\xi} = \pi_9\phi_1\phi_2[P_2 - \pi_5 P_1 - \pi_{15}\phi_2] - \pi_1 \frac{\phi_2 P_1^{\pi_4}}{r}. \tag{20}$$

The gas phase mass, momentum, and energy equations are replaced by mixture equations. The mixture mass, momentum, and energy equations are obtained by first adding the constituent mass, momentum, and energy equations (Eqs. 1 and 2, 3 and 4, and 5 and 6, respectively). These homogeneous equations then are integrated to form the algebraic mixture equations given below:

$$\rho_1\phi_1 v_1 + \frac{1}{\pi_5}\rho_2\phi_2 v_2 = -\pi_{18}, \tag{21}$$

$$\rho_1\phi_1 v_1^2 + P_1\phi_1 + \frac{1}{\pi_5}[\rho_2\phi_2 v_2^2 + P_2\phi_2] = \pi_{18} + \pi_{23}, \tag{22}$$

$$\rho_1\phi_1 v_1\left[e_1 + \frac{v_1^2}{2} + \frac{P_1}{\rho_1}\right] + \frac{1}{\pi_5}\rho_2\phi_2 v_2 \times \left[e_2 + \frac{v_2^2}{2} + \frac{P_2}{\rho_2}\right] = -\pi_{22}. \tag{23}$$

The number conservation equation is also homogeneous and thus is integrated to form an algebraic equation for particle radius:

$$r = \pi_{12}\sqrt[3]{\frac{-v_2\phi_2}{1-\pi_{11}}}. \tag{24}$$

The dimensionless gas and solid state equations and frozen sound speed definitions are

$$P_1 = [\pi_7 - 1]\rho_1 T_1[1 + \pi_{13}\rho_1], \tag{25}$$

$$e_1 = T_1, \tag{26}$$

$$\omega_1^2 = (\pi_7 - 1)T_1[1 + 2\pi_{13}\rho_1 + (\pi_7 - 1)(1 + \pi_{13}\rho_1)^2], \tag{27}$$

$$P_2 = [\pi_{17} - 1]\rho_2 T_2 - \pi_8, \tag{28}$$

$$e_2 = T_2 + \pi_8/\rho_2 + \pi_{10}, \tag{29}$$

$$\omega_2^2 = \pi_{17}(\pi_{17} - 1)T_2. \tag{30}$$

The saturation condition is unchanged in dimensionless form:

$$\phi_1 + \phi_2 = 1. \tag{31}$$

Undisturbed conditions for the four remaining ordinary differential equations are

$$\rho_2 = 1, \quad v_2 = -1, \quad T_2 = \pi_{14}, \quad \phi_2 = \pi_{20}. \tag{32}$$

It is next shown how the coupled set of differential-algebraic equations describing steady detonation structure (Eqs. 17-31) can be written as four differential equations in four unknowns—ρ_2, ϕ_2, v_2, and P_2—called the primary variables. First the mixture equations (Eqs. 21-23), state equations (Eqs. 25, 26, 28, and 29), and volume fraction definition (Eq. 31) can be used to write all gas phase variables in terms of the primary variables. By using Eqs. 25, 26, 28, and 29 to eliminate gas and solid energy in Eq. 23 and using Eq. 31 to eliminate gas volume fraction in Eqs. 21-23, Eqs. 21-23 can be rewritten as

$$\rho_1 v_1 = A(\rho_2, \phi_2, v_2, P_2), \tag{33}$$

$$P_1 + \rho_1 v_1^2 = B(\rho_2, \phi_2, v_2, P_2), \tag{34}$$

$$\rho_1 v_1\left(\frac{P_1}{(\pi_7 - 1)\rho_1(1 + \pi_{13}\rho_1)} + \frac{v_1^2}{2} + \frac{P_1}{\rho_1}\right) = C(\rho_2, \phi_2, v_2, P_2), \tag{35}$$

where A, B, C, and D are functions of the primary

variables as defined below:

$$A(\rho_2, \phi_2, v_2, P_2) = \frac{-\pi_{18} - (1/\pi_5)\rho_2\phi_2 v_2}{1-\phi_2}, \tag{36}$$

$$B(\rho_2, \phi_2, v_2, P_2) = \frac{\pi_{18} + \pi_{23} - (1/\pi_5)(\rho_2\phi_2 {v_2}^2 + P_2\phi_2)}{1-\phi_2}, \tag{37}$$

$$C(\rho_2, \phi_2, v_2, P_2) = \frac{-\pi_{22} - \frac{1}{\pi_5}\rho_2\phi_2 v_2\left[\frac{P_2 + \pi_{17}\pi_8}{(\pi_{17}-1)\rho_2} + \pi_{10} + \frac{{v_2}^2}{2} + \frac{P_2}{\rho_2}\right]}{1-\phi_2}. \tag{38}$$

Equations 33–35 can be combined to form a cubic equation for gas density. This is done by first using Eq. 33 to express gas velocity as a function of gas density and solid variables. Then gas velocity may be eliminated from Eqs. 34 and 35. Thus modified, Eq. 34 can be used to express gas pressure as a function of gas density and solid variables. This result is used to eliminate gas pressure from the modified energy equation (Eq. 35). The resulting equation is a cubic equation for gas density whose coefficients are functions of the primary variables

$$\begin{aligned}&[-2(\pi_7-1)\pi_{13}C]{\rho_1}^3 + [2(\pi_7-1)\\ &\times (AB\pi_{13} - C)]{\rho_1}^2\\ &+ [2AB\pi_7 - (\pi_7-1)A^3\pi_{13}]\rho_1\\ &- [(\pi_7+1)A^3] = 0.\end{aligned} \tag{39}$$

Equation 39 can be solved exactly for gas density in terms of the primary variables. An explicit but lengthy solution to Eq. 39 can be written using the general cubic equation solution. Three solutions for Eq. 39 exist. One is associated with a shocked gas, another is associated with an unshocked gas, and the third predicts a negative density for all cases studied and is thus unphysical. This extraneous root is present only when nonideal gas effects are included. (It is seen from Eq. 39 that for no nonideal effects, $\pi_{13} = 0$, the equation is quadratic, and only two solutions exist.) It is possible for Eq. 39 to predict a pair of imaginary roots under certain conditions. If such a condition is reached, the reaction zone structure is unphysical.

With the gas density predicted from Eq. 39 as a function of the primary variables, all other gas phase variables can be expressed as functions of the primary variables. The gas velocity is found by using Eq. 33. The gas pressure can then be determined from Eq. 34 and the gas energy, temperature, and sound speed from Eqs. 25–27.

It is now shown how to uncouple the differential equations (Eqs. 17–20). Equations 17–20 can be expressed in the form

$$A_{ij}\frac{du_j}{d\xi} = B_i, \tag{40}$$

where $u_j = (\rho, \phi_2, v_2, P_2)$ and A_{ij} and B_i are functions of the primary variables. To put the equations in a form suitable for phase space analysis, explicit expressions for the derivatives $du_j/d\xi$ must be obtained. This is done by applying the inverse operator ${A_{ij}}^{-1}$ to Eq. 40.

$$\frac{du_i}{d\xi} = {A_{ij}}^{-1}B_j \tag{41}$$

A necessary step to express Eqs. 17–20 in this form is to use the solid state equations (Eqs. 28 and 29) to determine an expression for the derivative of solid energy in terms of solid pressure and density. Equation 28 can be used to eliminate solid temperature from Eq. 29 so that this derivative can be determined.

$$\frac{de_2}{d\xi} = \frac{1}{(\pi_{17}-1)\rho_2}\frac{dP_2}{d\xi} - \frac{P_2 + \pi_{17}\pi_8}{(\pi_{17}-1){\rho_2}^2}\frac{d\rho_2}{d\xi}. \tag{42}$$

Expanding the derivative in Eq. 17 and using Eq. 42 allows Eqs. 17–20 to be written as a system

in the form of Eq. 40:

$$\begin{bmatrix} \phi_2 v_2 & \rho_2 v_2 & \rho_2 \phi_2 & 0 \\ 0 & P_2 & \rho_2 \phi_2 v_2 & \phi_2 \\ -\dfrac{P_2 + \pi_{17}\pi_8}{(\pi_{17}-1)\rho_2} v_2 & 0 & P_2 & \dfrac{v_2}{(\pi_{17}-1)} \\ 0 & v_2 & 0 & 0 \end{bmatrix} \begin{bmatrix} \dfrac{d\rho_2}{d\xi} \\ \dfrac{d\phi_2}{d\xi} \\ \dfrac{dv_2}{d\xi} \\ \dfrac{dP_2}{d\xi} \end{bmatrix}$$

$$= \begin{bmatrix} -\pi_1 \rho_2 \phi_2 {P_1}^{\pi_4}/r \\ -\pi_2 (v_2 - v_1)\phi_1 \phi_2 / r \\ -\pi_3 (\pi_6 T_2 - T_1)\phi_1 / r^{1/3} \\ \pi_9 \phi_1 \phi_2 (P_2 - \pi_5 P_1 - \pi_{15}\phi_2) - \pi_1 \phi_2 {P_1}^{\pi_4}/r \end{bmatrix}. \tag{43}$$

The left-hand side of Eq. 43 is expressed in terms of the primary variables. Using previous algebraic relations, the right-hand side can also be expressed in terms of these variables. By applying the inverse operator explicit expressions can be obtained for the derivatives of the fundamental variables.

$$\frac{d\rho_2}{d\xi} = \frac{D\left[\dfrac{\rho_2 {v_2}^2}{\pi_{17}-1} - P_2\right] - E\left[\dfrac{\rho_2 v_2}{\pi_{17}-1}\right] + F[\rho_2]}{\dfrac{\rho_2 v_2}{\pi_{17}-1}\left({v_2}^2 - \pi_{17}\dfrac{P_2 + \pi_8}{\rho_2}\right)}, \tag{44}$$

$$\frac{d\phi_2}{d\xi} = \pi_9 \frac{\phi_1 \phi_2}{v_2}[P_2 - \pi_5 P_1 - \pi_{15}\phi_2] - \pi_1 \frac{\phi_2 {P_1}^{\pi_4}}{v_2 r}, \tag{45}$$

$$\frac{dv_2}{d\xi} = \frac{-D\left[\dfrac{P_2 + \pi_{17}\pi_8}{(\pi_{17}-1)\rho_2} v_2\right] + E\left[\dfrac{{v_2}^2}{\pi_{17}-1}\right] - F[v_2]}{\dfrac{\rho_2 v_2}{\pi_{17}-1}\left({v_2}^2 - \pi_{17}\dfrac{P_2 + \pi_8}{\rho_2}\right)}, \tag{46}$$

$$\frac{dP_2}{d\xi} = \frac{D\left[\dfrac{P_2 + \pi_{17}\pi_8}{\pi_{17}-1} {v_2}^2\right] - E\left[P_2 v_2 + \dfrac{P_2 + \pi_{17}\pi_8}{\pi_{17}-1} v_2\right] + F[\rho_2 {v_2}^2]}{\dfrac{\rho_2 v_2}{\pi_{17}-1}\left[{v_2}^2 - \pi_{17}\dfrac{P_2 + \pi_8}{\rho_2}\right]}, \tag{47}$$

where D, E, and F are defined as follows:

$$D = -\pi_9 \rho_2 \phi_1 (P_2 - \pi_5 P_1 - \pi_{15}\phi_2), \tag{48}$$

$$E = -\pi_2 (v_2 - v_1)\frac{\phi_1}{r} + \frac{P_2}{v_2} \times \left[\pi_1 \frac{{P_1}^{\pi_4}}{r} - \pi_9 \phi_1 (P_2 - \pi_5 P_1 - \pi_{15}\phi_2)\right], \tag{49}$$

$$F = -\pi_3 (\pi_6 T_2 - T_1)\frac{\phi_1}{r^{1/3}}. \tag{50}$$

Equations 44, 46, and 47 are singular when the following condition is met:

$${v_2}^2 = \pi_{17}\frac{P_2 + \pi_8}{\rho_2}. \tag{51}$$

By using the solid thermal state equation (Eq.

28) to eliminate solid pressure and density in favor of solid temperature and using the solid sound speed definition (Eq. 30), Eq. 51 can be rewritten as

$$v_2^2 = \omega_2^2. \tag{52}$$

Thus when the velocity of the solid relative to the wave head equals the local frozen solid sound speed, the system of Eqs. 43 is singular. It is seen by examination of Eqs. 49 and 50 that the equations are also singular at the complete reaction state because the particle radius r appears in the denominator of the expressions for E and F. Near these singularities, numerical methods are unable to calculate the derivatives in ξ space.

In general, steady two-phase systems of the form given in Eqs. 1–14 of Ref. 16, that is for general state equations, have singularities in derivatives when either the gas velocity equals the local frozen gas sound speed or the solid velocity equals the local frozen solid sound speed. This can be shown by writing the full steady two-phase equations in matrix form similar to Eq. 43. The derivatives are singular whenever the determinant of the coefficient matrix is zero. It is easily shown that this occurs when either phase is locally sonic.

A transformation of independent variables can be devised to effectively remove the difficulties associated with the solid sonic singularity and complete reaction singularity. By defining a new independent variable z such that

$$\frac{d\xi}{dz} = r(v_2^2 - \omega_2^2) \qquad \text{with} \quad \xi(z=0) = 0, \tag{53}$$

and multiplying Eqs. 44–47 by Eq. 53, Eqs. 44–47 are transformed into four ordinary differential equations with z rather than ξ as the independent variable. These transformed equations are not singular at complete reaction or a solid sonic condition. However, they contain the added complexity of an additional differential equation.

SHOCK DISCONTINUITIES

As in one-phase ZND theory, one must consider shock discontinuities when analyzing two-phase detonations. The shock state is not an equilibrium state and can serve as an initiation mechanism for chemical reaction. In this model a shock wave is modeled as an infinitely thin zone where all flow variables change values discontinuously. Such discontinuities are admitted by the governing equations because they are hyperbolic. In this analysis mechanisms that would define a shock structure such as diffusive energy and momentum transport have been neglected. It is assumed that the length scales where these processes are important are much smaller than the length scales associated with chemical reaction, interphase drag, heat transfer, and compaction.

The shock equations can be derived by considering Eqs. 1–7. Through the shock discontinuity, reaction, drag, heat transfer, and compaction processes have no time to occur and may thus be neglected. By neglecting these terms, a discontinuity analysis provides the following jump conditions:

$$[\rho_1 \phi_1 v_1] = 0, \tag{54}$$

$$[\rho_2 \phi_2 v_2] = 0, \tag{55}$$

$$[\rho_1 \phi_1 v_1 + P_1 \phi_1] = 0, \tag{56}$$

$$[\rho_2 \phi_2 v_2 + P_2 \phi_2] = 0, \tag{57}$$

$$[\rho_1 \phi_1 v_1 (e_1 + v_1^2/2 + P_1/\rho_1)] = 0, \tag{58}$$

$$[\rho_2 \phi_2 v_2 (e_2 + v_2^2/2 + P_2/\rho_2)] = 0, \tag{59}$$

$$[\phi_2] = 0. \tag{60}$$

Here the brackets denote a jump condition as defined below for the general variable ψ:

$$[\psi] = \psi(\text{shocked state}) - \psi(\text{ambient state}). \tag{61}$$

From Eq. 60 it is seen that the volume fraction does not change through a shock discontinuity. Using this result, the gas shock equations (Eqs. 54, 56, and 58) along with gas phase state equations are sufficient to determine the gas shock state. The solid shock equations (Eqs. 55, 57, and 59) along with the solid phase state equations are sufficient to solve for the solid shock state. When the con-

stant factor of volume fraction is removed from these equations, they are identical to two sets of one-phase shock equations. The shock state for the gas and solid are thus identical to their one-phase equivalents. Detailed equations for the two-phase shock state are reported in Ref. 11. Four physical states are admitted by the shock discontinuity equations: (1) shocked gas, shocked solid, (2) unshocked gas, shocked solid, (3) shocked gas, unshocked solid, and (4) unshocked gas, unshocked solid.

TWO-EQUATION MODEL

In certain limits the two-phase equations can be reduced to two autonomous ordinary differential equations in two unknowns. These limits are taken for purely mathematical reasons and are not motivated by physical considerations. Reduction to two differential equations allows one to use an easily understood two-dimensional phase plane to study the trajectories of the integral curves. To derive the two-equation model, one must consider the zero-compaction, zero-heat transfer limit, corresponding to $\pi_9 \to 0$, $\pi_3 \to 0$. In this limit, Eqs. 48 and 50 hold that $D = F = 0$. Then if Eq. 44 (transformed to z space) is multiplied by solid velocity and added to the product of solid density and Eq. 46 (also transformed to z space), the following homogeneous equation is obtained:

$$v_2 \frac{d\rho_2}{dz} + \rho_2 \frac{dv_2}{dz} = 0. \tag{62}$$

This equation can be integrated to form the algebraic relation

$$\rho_2 v_2 = -1. \tag{63}$$

In applying the initial conditions when integrating this equation, it is unnecessary to specify whether the initial state is shocked or unshocked. This arises because Eq. 63 is equivalent to the shock relation (Eq. 55) when it is recalled that volume fraction does not change through the shock discontinuity.

To determine a second algebraic relation, Eq. 63 must first be used to eliminate solid velocity in favor of solid density in all remaining equations. Then if Eq. 47 (in z space) is multiplied by the factor

$$\frac{1}{{\rho_2}^{\pi_{17}}}$$

and added to the product of the z-space Eq. 44 and the factor

$$-\pi_{17}\frac{P_2 + \pi_8}{{\rho_2}^{\pi_{17}+1}},$$

the following homogeneous equation is obtained:

$$\frac{1}{{\rho_2}^{\pi_{17}}}\frac{dP_2}{dz} - \pi_{17}\frac{P_2 + \pi_8}{{\rho_2}^{\pi_{17}+1}}\frac{d\rho_2}{dz} = 0. \tag{64}$$

This equation may be integrated to form an algebraic relation between solid pressure and density. The constant of integration for this expression is dependent on whether the initial state is shocked or unshocked. Thus

$$P_2 = K{\rho_2}^{\pi_{17}} - \pi_8, \tag{65}$$

with

$$K = \begin{cases} \dfrac{2 - \pi_{14}(\pi_{17} - 1)^2}{\pi_{17} + 1}\left[\dfrac{(\pi_{17} - 1)(1 + 2\pi_{14}\pi_{17})}{(\pi_{17} + 1)}\right]^{\pi_{17}}, & \text{shocked solid} \\ \pi_{21} + \pi_8. & \text{unshocked solid} \end{cases}$$

When Eqs. 63 and 65 are used to eliminate solid velocity and pressure from Eqs. 44 and 45, the two-equation model is found:

$$\begin{aligned} \frac{d\rho_2}{dz} &= \pi_2(v_1 - v_2){\rho_2}^2\phi_1 \\ &\quad - (K{\rho_2}^{\pi_{17}} - \pi_8)\pi_1{\rho_2}^3{P_1}^{\pi_4} \\ &= f(\rho_2, \phi_2), \end{aligned} \tag{66}$$

$$\begin{aligned} \frac{d\phi_2}{dz} &= \pi_1\rho_2\phi_2{P_1}^{\pi_4}(\pi_{17}K{\rho_2}^{\pi_{17}+1} - 1) \\ &= h(\rho_2, \phi_2), \end{aligned} \tag{67}$$

with

$$\frac{d\xi}{dz} = r(\pi_{17}K{\rho_2}^{\pi_{17}+1} - 1) = g(\rho_2, \phi_2). \tag{68}$$

Equations 66 and 67 are autonomous in ρ_2 and ϕ_2, as all other variables can be expressed as functions of ρ_2 and ϕ_2. Equation 68 may be thought of as an auxiliary equation to determine the distance variable ξ once the structure predicted by Eqs. 66 and 67 has been determined. The forcing functions in Eqs. 66–68 are defined above as f, g, and h.

EQUILIBRIUM END STATE ANALYSIS

Before considering detonation structure, equilibrium end states should be considered. This analysis can be performed without regard to structure and identifies the point that the solution much reach. An equilibrium end state exists when the forcing functions of the ordinary differential equations are simultaneously zero. One potential equilibrium end state is the complete reaction state ($r = \phi_2 = 0$). For the two equation model at this state Eq. 67 predicts equilibrium. Equation 66 yields an algebraic condition for solid density at equilibrium. In setting $f(\rho_2, 0) = 0$, one algebraic equation to be solved for solid density is obtained. As all other variables are functions of solid density and volume fraction, the equilibrium end state is completely specified by this condition. It is also noted that at the complete reaction end state Eq. 68 is in equilibrium. The complete reaction solid end state has not been determined algebraically for the four-equation model. It has been found by integrating the full four-equation model that a well-defined, bounded equilibrium end state exists.

At the compete reaction end state, the mixture equations (Eqs. 21–23) and gas phase state equations (Eqs. 25 and 26) completely describe the gas phase. Furthermore, at the complete reaction state, the gas phase is independent of the solid state as long as the solid end state is finite. As described in detail in Refs. 11 and 15, it is possible to derive two-phase equivalents to the Rayleigh line and Hugoniot equations of one-phase flow at the complete reaction state (and only at the complete reaction state). It is then possible to describe the two-phase CJ condition, the state at which the gas velocity is equal to the gas sound speed. Because the CJ condition is a sonic condition, it can be argued, as for one-phase CJ theory, that the CJ wave speed is the unique speed of propagation for a two-phase detonation with no piston support. Because the end point of the reaction is traveling at a sonic speed, no rarefaction waves downstream of the reaction zone can catch and interfere with the reaction zone. For wave speeds greater than CJ wave speeds, two physical solutions are possible. One corresponds to the strong detonation solution and the other corresponds to the weak solution of one-phase CJ theory. As for one-phase theory, the gas velocity at the strong point is subsonic; thus, the wave requires piston support to propagate. At the weak point, the gas velocity is supersonic; thus, this point cannot be ruled out by equilibrium end state analysis.

STRUCTURE ANALYSIS

In this section reaction zone structure predicted by the two- and four-equation models is considered. Most of the discussion refers to the two-equation model because of its relative simplicity. Predictions of the full model equations are compared to the two-equation model predictions.

Whether Eqs. 66 and 67 should be integrated forward or backward in z is a relevant question. The equations should be integrated so that ξ goes from 0 to $-\infty$. From Eq. 68 it is seen that the direction of change of ξ with respect to z depends on whether the solid phase is subsonic or supersonic. If the initial state of the solid is unshocked, the solid is locally supersonic, $g > 0$, and a negative dz corresponds to a negative $d\xi$. If the initial state of the solid is shocked, the flow is locally subsonic, $g < 0$, and a positive dz must be chosen to recover a negative $d\xi$.

There are several requirements for an admissible detonation structure. An admissible steady structure is defined by an integral curve that begins at the initial point in the ρ_2–ϕ_2 plane and travels in that plane to an equilibrium position where f and h are simultaneously zero. In addition further restrictions are placed on the solution. It is required that the gas and solid thermodynamic variables density, pressure, and temperature are always positive and real. Also it is required that all physical variables are single-valued functions of the position variable ξ. Based on these restric-

tions parametric conditions can be obtained for admissibility of a detonation solution.

The conditions under which thermodynamic variables become either negative or imaginary are checked numerically. By examining a few limited cases, it has been found that there are regions in the ρ_2-ϕ_2 plane where gas phase pressure, density, and temperature are negative. In solving the cubic equation for the gas properties, imaginary gas phase quantities are sometimes predicted. It has been found numerically that the border of the imaginary region corresponds to a sonic condition in the gas phase. This result is suggested by the fact that the more general differential equations (Eqs. 1-8) are singular when the gas velocity equals the local gas sound speed.

The geometry of the $f = 0$ and $h = 0$ curves is critical in determining the integral curve that defines the steady-state solution. Depending on the relative orientation of these curves and the initial state, many classes of solutions exist, each with a distinct character. Some solutions reach an equilibrium state, defined at the intersection of the $f = 0$ and $h = 0$ curves. The existence conditions for a steady detonation solution are strongly influenced by the nature of the equilibrium point, which can be classified as a source, sink, saddle, or spiral. For example, if the equilibrium point to which the integral curve is drawn is a sink, then it is relatively easy to find steady solutions as all integral curves in the neighborhood of the sink are attracted to the sink. If, however, the equilibrium point is a saddle, solutions are more difficult to find; usually special conditions are required for such solutions. For some wave speeds the orientation of the $f = 0$ and $h = 0$ curves prevents solutions from reaching an equilibrium state; these solutions cannot be classified as steady solutions. Among these types of solutions are those that pass through a solid sonic point and become physically unacceptable, multivalued functions of distance.

Figure 1 shows sketches of phase planes for two classes of solutions, one an acceptable detonation structure, the other a nonphysical solution. Each sketch shows the separatrix lines $f = 0$ and $g = h = 0$. The equilibrium position is at the intersection of these curves. Each curve shows a solid phase sonic line, $g = h = 0$, forbidden regions in which gas phase properties are not physical, and integral curves that originate from the initial condition. For the acceptable structure the integral curve travels from the initial state to the equilibrium position. By changing the flow conditions, the topology of this phase plane is altered, shown in the adjacent sketch. In this sketch, the integral curve is driven through the solid sonic line and is incapable of reaching the equilibrium point. As explained below, past the solid sonic line, the solution is double-valued and therefore not physical.

Thermodynamic variables become double-valued functions of distance when a solid sonic condition ($g = 0$) is reached at a nonequilibrium point in the phase plane ($f \neq 0$). From Eq.

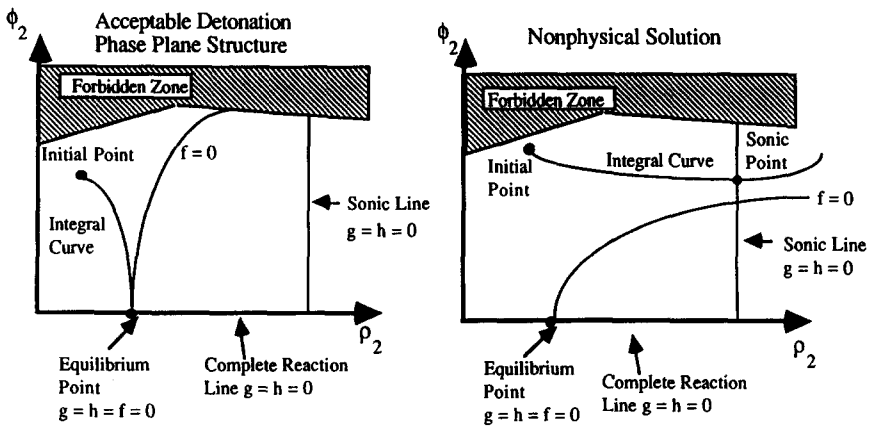

Fig. 1. Phase plane sketches of physical and nonphysical solutions.

68, it is seen that the direction of change of ξ with respect to z changes when the solution passes through a solid sonic point. Thus ξ, which starts at zero and moves towards $-\infty$ as reaction progresses, changes direction and moves towards $+\infty$ at a critical point ξ_{min} when a solid sonic condition is reached. Through this point Eqs. 66 and 67 predict a continuous variation of density and volume fraction. At the solid sonic point the derivatives of ρ_2 and ϕ_2 with respect to z are finite, and the derivatives with respect to ξ are infinite. At any given location ξ, $\xi > \xi_{min}$, two values of each thermodynamic variable will be predicted.

Results analogous to one-phase ZND theory can be obtained with the two-equation model. For the input conditions of Table 1, with the heat transfer coefficient $h = 0$ and compaction viscosity $\mu_c \to \infty$, an initial solid volume fraction greater than 0.19, and an initially shocked gas and unshocked solid, a CJ detonation structure can be defined. In these limits there is no heat transfer or volume fraction change due to compaction.

The ordinary differential equations of the two-equation model and full, four-equation model were solved numerically. Integration was performed using the IMSL subroutine DVERK, a fifth- and sixth-order Runge-Kutta routine, on the UIUC Cyber 175. Step sizes were chosen such that none of the fundamental variables, ρ_2, ϕ_2, v_2, and P_2, changed by more than 5% in value in any given integration step. Typically about 200 integration steps were sufficient to describe the reaction zone. A typical integration took 20 CPU seconds to complete.

For an initial solid volume fraction of 0.70, Fig. 2 shows a plot of the phase plane for a CJ wave speed of 7369 m/s. This curve shows the sonic line ($g = h = 0$) on $\rho_2 = 1.35$, the complete reaction line ($g = h = 0$) on $\phi_2 = 0$, and the $f = 0$ line. It is seen from this curve that the only equilibrium point is at $(\rho_2, \phi_2) = (1.04, 0)$. The vector field superimposed in Fig. 2, defined by Eqs. 66 and 67, indicates that this point is a sink that is confirmed by a local linear analysis near the equilibrium point. The integral curve connecting the initial state to the equilibrium point is also plotted

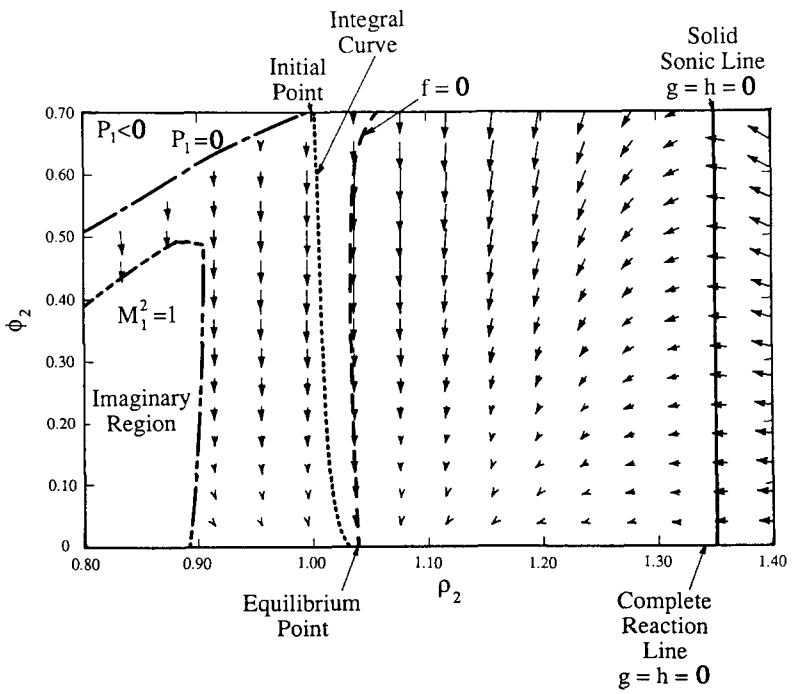

Fig. 2. Phase plane for CJ detonation with leading gas phase shock.

in Fig. 2. This curve is obtained by numerical integration of Eqs. 66 and 67. This integral curve moves in a direction defined by the vector field of the phase plane. Curves of zero gas phase pressure are plotted in Fig. 2 along with the curve defining the boundary between pure real and imaginary gas phase quantities. The gas velocity is locally sonic ($M_1^2 = 1$) on the boundary of the region where imaginary gas phase properties exist.

When the full model equations are considered, general results from the two-equation model are retained. It is more difficult to interpret these results as the phase space is four dimensional. With a given set of initial conditions, the gas phase CJ end state is the same whether the two- or four-equation model is used. The solid phase end state and details of the reaction zone structure do depend on which model equations are used. Plots of predicted detonation structure are shown in Fig. 3, which contains plots of solid and gas density, lab velocity u, pressure, temperature, Mach number, particle radius, and solid volume fraction versus distance ξ. Also plotted in Fig. 3 are results from the two-equation model. It is seen that both models predict results of the same order of magnitude. Gas phase quantities are nearly identical for both models. Although there are small differences in solid phase predictions, these results are remarkable as there is no real basis to assume that the limits taken are appropriate for this class of models. These results suggest that in a limited region of parameter space, material compaction and heat transfer are not important mechanisms in determining two-phase detonation structure. Thus there is some justification in using the two-equation model as a tool for understanding the full model equations. A comparison of some results of the two models is given in Table 2.

In Fig. 3 it is seen that the gas phase is shocked whereas the solid phase is unshocked. It is seen from Fig. 3e that the gas pressure continues to rise past the initial shocked gas pressure. This is in contrast to one-phase ZND theory, which predicts the pressure to be a maximum at the shock state. The high gas phase temperature ($\sim 10,000$ K) indicates that ionization, dissociation, and radiative heat transfer could be important mechanisms in the reaction zone.

Nonphysical solutions are now considered. Such solutions exist below a critical value of initial solid volume fraction for a structure with a single leading gas phase shock and unshocked solid. The critical point is shown in Fig. 4, which plots CJ wave speed versus initial bulk density ρ_a ($\rho_a = \rho_{10}\phi_{10} + \rho_{20}\phi_{20}$). Figure 4 also compares predictions of this model with those of the unsteady model of Butler and Krier [5] and those of the equilibrium thermochemistry code TIGER given in Ref. 5. The feature of a critical initial bulk density has not been identified by other models. It is emphasized that an algebraic end state analysis does not rule out solutions below the critical initial bulk density. Only when the structure is examined are such solutions ruled out.

For a value of initial solid volume fraction of 0.20, very near the critical bulk density, an acceptable detonation structure is obtained. A phase portrait, vector map, and integral curve is shown in Fig. 5. Figure 5 resembles Fig. 2, but the curves have all been skewed. Note that the integral curve nearly reaches the sonic state before turning around and traveling to the complete reaction end state.

For an initial solid volume fraction of 0.15, a nonphysical solution is obtained for a CJ wave speed and an initial lead shock in the gas and unshocked solid. The two-equation model's phase plane is shown in Fig. 6. The integral curve in this plane passes through the solid sonic line at a nonequilibrium point, causing the solution to become double-valued. A plot of the solid phase Mach number is shown in Fig. 7 for both the two- and four-equation models. Again both models predict nearly identical results. It is seen from Fig. 7 that infinite gradients with respect to ξ are predicted precisely at the point where the solid phase reaches a sonic velocity ($M_2^2 = 1$).

Solutions with no leading shock in either the gas or solid phase are also admitted by this model. Figure 8 shows the phase portrait, vector map, and integral curve for a CJ wave with no leading gas or solid shock propagating through a mixture with an initial solid volume fraction of 0.70. Again, the equilibrium point is a sink. As summarized in Table 2, the main difference between this case and the case with the leading gas phase shock is

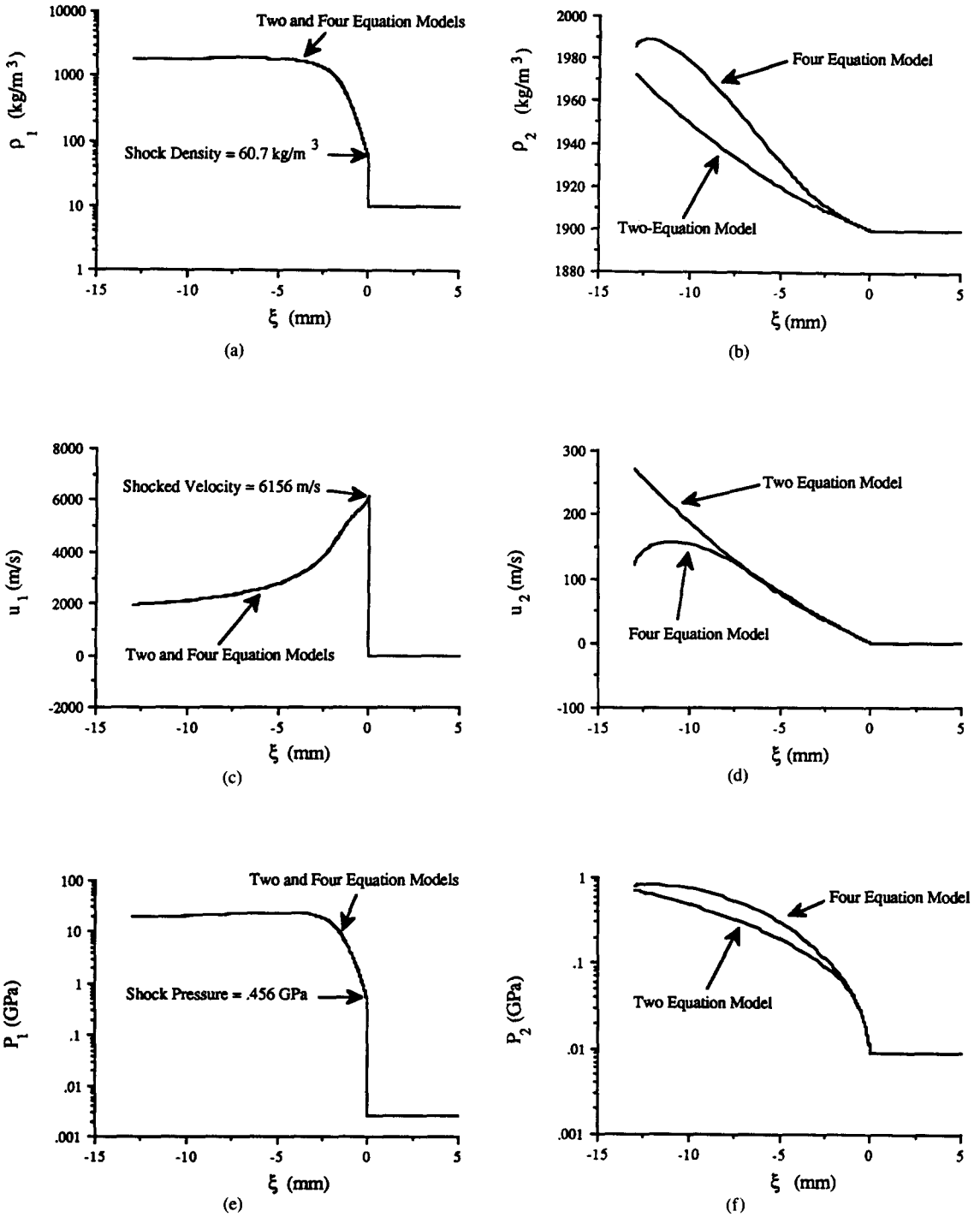

Fig. 3. (a, b) Gas and solid density CJ detonation structure. (c, d) Gas and solid velocity CJ detonation structure. (e, f) Gas and solid pressure CJ detonation structure. (g, h) Gas and solid temperature CJ detonation structure. (i, j) Gas and solid Mach number squared CJ detonation structure. (k, l) Solid volume fraction and particle radius CJ detonation structure.

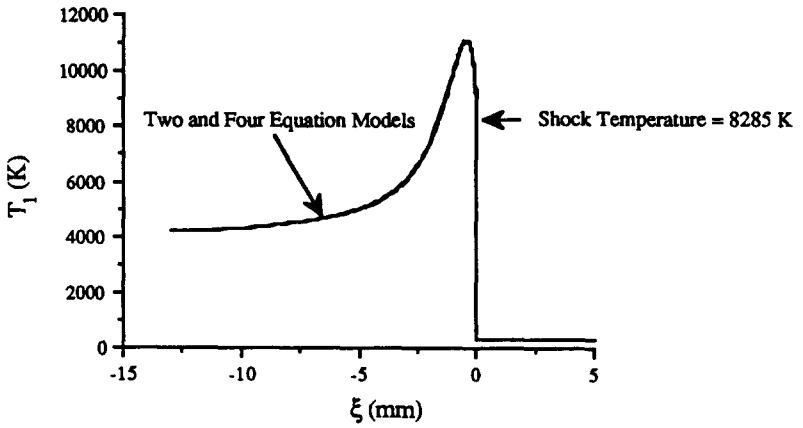

(g)

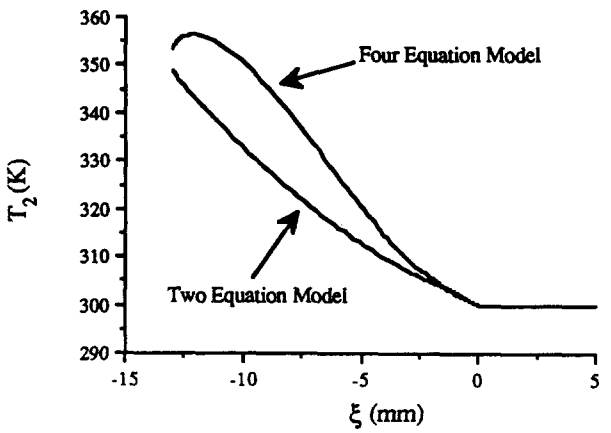

(h)

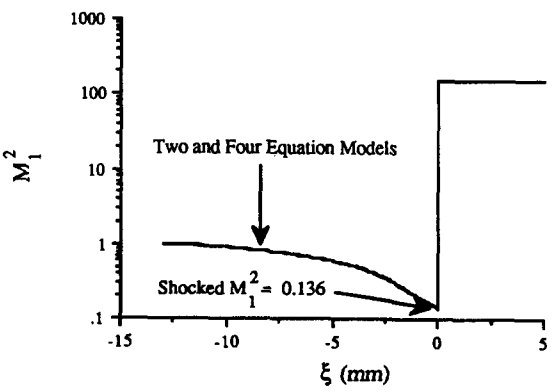

(i)

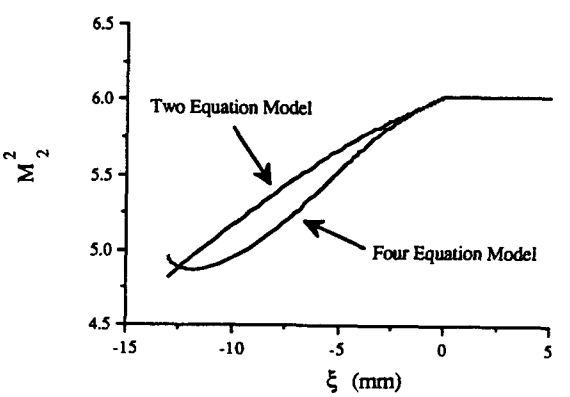

(j)

Fig. 3 (continued).

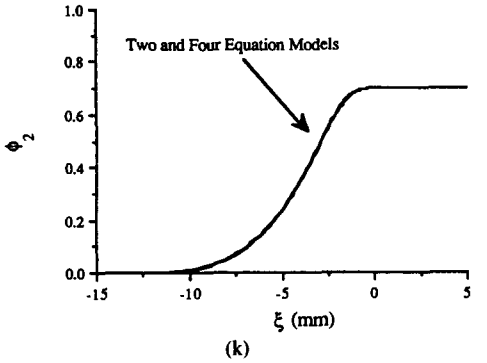

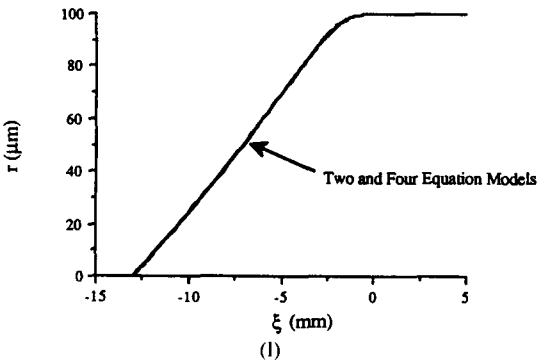

Fig. 3 (continued).

that the reaction zone is much longer (62 vs. 13 mm). Again both two- and four-equation models predict similar results. The CJ gas phase end state is identical regardless of whether the initial gas state is shocked or unshocked, or whether the two- or four-equation model is used. This is because the complete reaction CJ state is independent of the structure of the detonation. Small differences in the CJ temperatures and gas velocities are due to numerical roundoff errors. In general the solid end state can vary for each state presented in Table 2. The solid phase end state predicted by the two-equation model is nearly the same for both the unshocked and shocked gas, as is the solid phase end state for the four-equation model.

For wave speeds greater than CJ, strong and weak waves can be predicted. For an initial solid volume fraction of 0.70, a wave speed of 8000 m/s (which is greater than the CJ wave speed of 7369 m/s), and an unshocked solid, Figs. 9 and 10 show plots of the two-equation model's phase portraits for the strong (initially shocked gas) and weak (initially unshocked gas) case. The equilibrium points are sinks in both cases. The results of

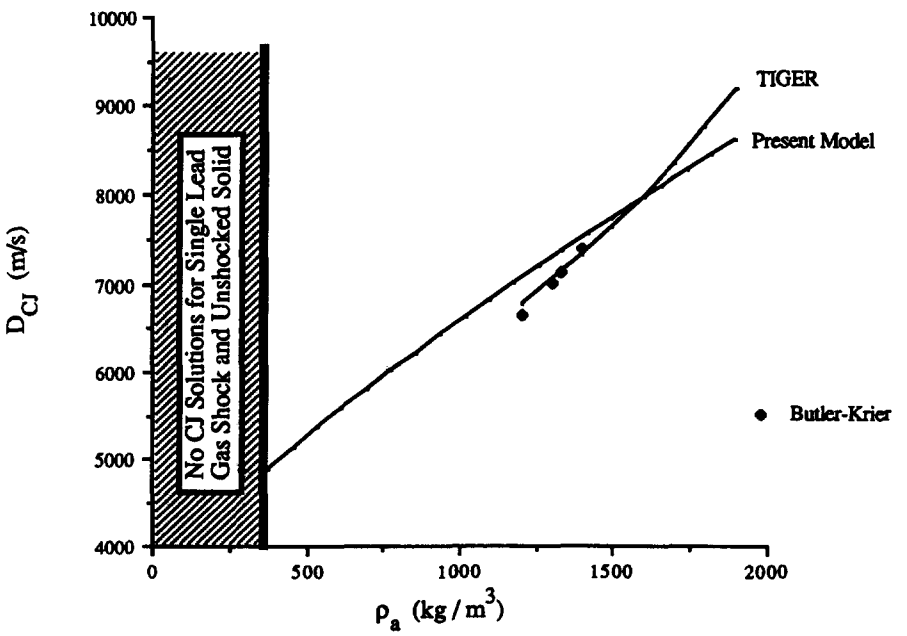

Fig. 4. CJ wave speed vs. initial bulk density.

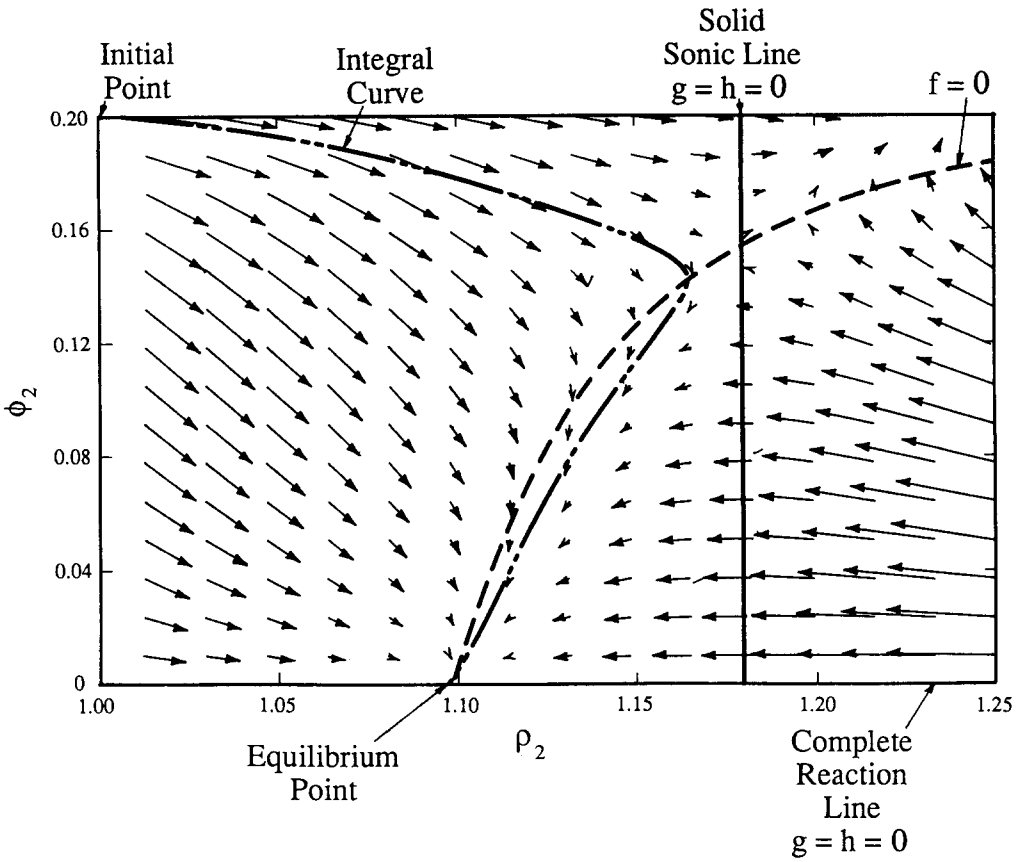

Fig. 5. Phase plane for CJ detonation near critical initial bulk density.

TABLE 2

Comparison of Two- and Four-Equation Model Predictions for CJ Waves With and Without Leading Gas Phase Shock

	Leading Gas Shock		*No Leading Gas Shock*	
	Two-Equation	*Full*	*Two-Equation*	*Full*
Initial bulk density	1,333 kg/m^3	1,333 kg/m^3	1,333 kg/m^3	1,333 kg/m^3
Reaction zone length	13.0 mm	13.0 mm	62.1 mm	62.2 mm
CJ wave speed	7,369 m/s	7,369 m/s	7,369 m/s	7,369 m/s
CJ pressure	19.4 GPa	19.4 GPa	19.4 GPa	19.4 GPa
CJ density	1,821 kg/m^3	1,821 kg/m^3	1,821 kg/m^3	1,821 kg/m^3
CJ temperature	4,176 K	4,176 K	4,174 K	4,174 K
CJ gas velocity	1,976 m/s	1,976 m/s	1,974 m/s	1,974 m/s
(CJ gas Mach number)^2	1	1	1	1
Maximum gas temperature	11,119 K	11,120 K	4,174 K	4,174 K
Final solid pressure	0.716 GPa	0.796 GPa	0.716 GPa	0.797 GPa
Final solid density	1,973 kg/m^3	1,985 kg/m^3	1,973 kg/m^3	1,985 kg/m^3
Final solid temperature	349 K	353 K	349 K	353 K
Final solid velocity	272 m/s	121 m/s	272 m/s	120 m/s
(Final solid Mach number)^2	4.82	4.96	4.82	4.96

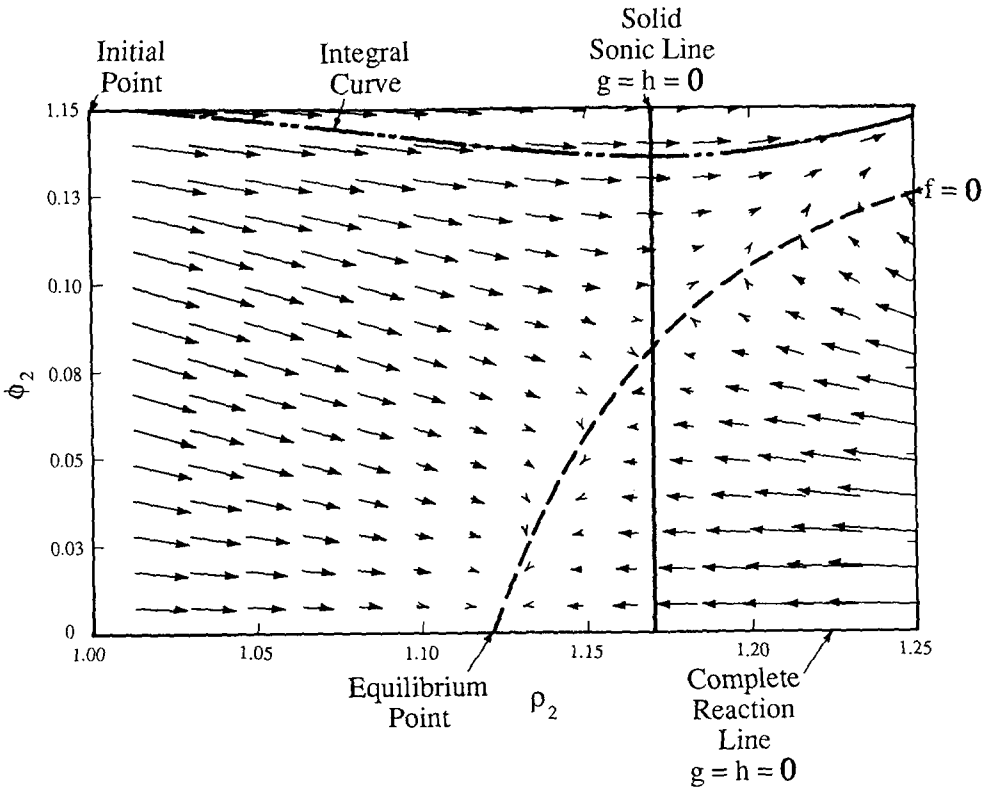

Fig. 6. Phase plane for non-physical solution.

these calculations for both two- and four-equation models are summarized in Table 3. For the strong case the reaction zone is shorter than for the corresponding CJ wave with a leading gas phase shock. For the weak case the reaction zone is longer than for the corresponding CJ wave without a leading gas phase shock. Again two- and four-equation models predict similar results.

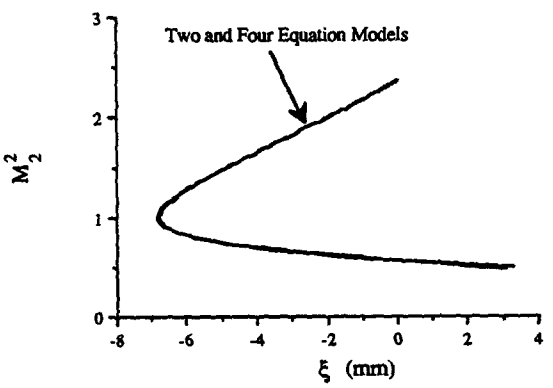

Fig. 7. Non-physical two-phase structure.

A continuum of two-phase detonation wave speeds as a function of piston velocity is predicted. Detonation wave speed is plotted as a function of piston velocity in Fig. 11. For wave speeds greater than CJ, piston support is required to support the wave. The CJ wave can propagate with or without piston support as the complete reaction point is a gas phase sonic point. For piston velocities below CJ, a continuum of weak waves are predicted. The implications of this are unclear. As the complete reaction point is supersonic, the piston support is not necessary. This suggests that the solution may not be unique. Simple one-phase ZND theory also predicts a continuum of weak waves. Fickett and Davis [14] discuss this issue for one-phase theory. Although this issue is still not settled for the one-phase model, some have suggested that the weak waves may be ruled out as unphysical because of a lack of an initiation mechanism. Fickett and Davis

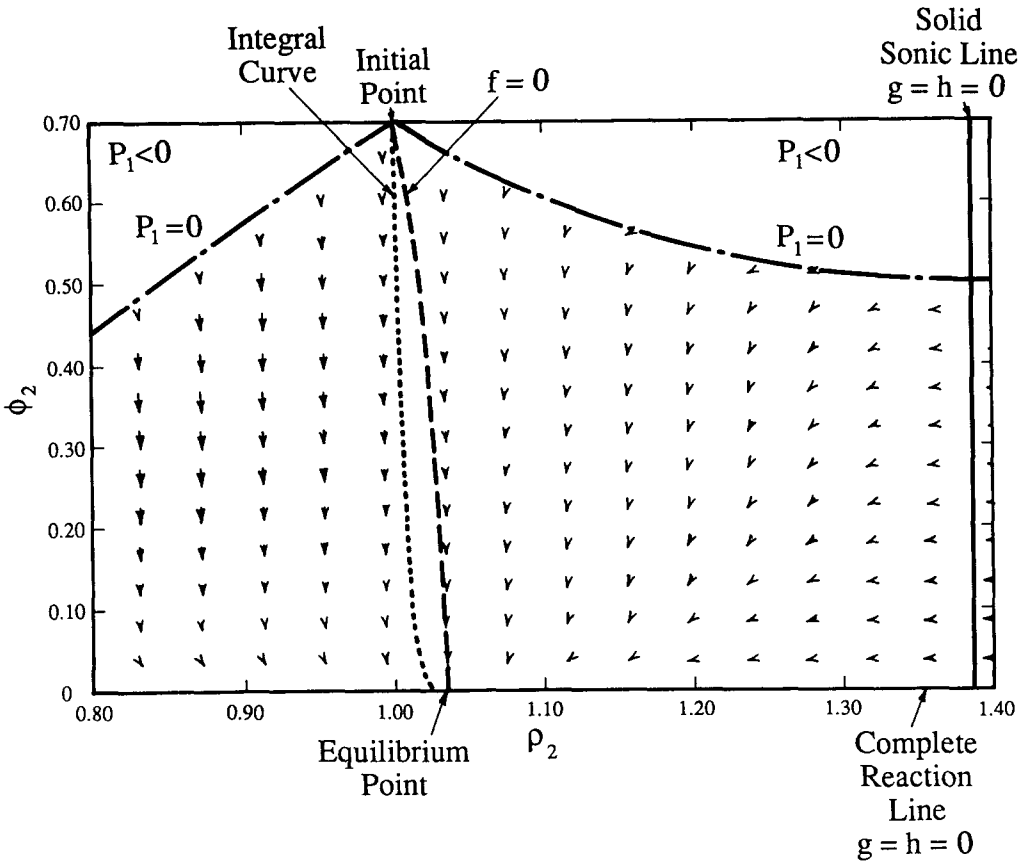

Fig. 8. Phase plane for CJ detonation with no leading gas phase shock.

TABLE 3

Comparison of Two- and Four-Equation Model Predictions for Strong and Weak Detonations, D = 8,000 m/s

	Leading Gas Shock (Strong)		*No Leading Gas Shock (Weak)*	
	Two-Equation	*Full*	*Two-Equation*	*Full*
Initial bulk density	1,333 kg/m^3	1,333 kg/m^3	1,333 kg/m^3	1,333 kg/m^3
Reaction zone length	10.2 mm	10.2 mm	71.4 mm	71.5 mm
Wave speed	8,000 m/s	8,000 m/s	8,000 m/s	8,000 m/s
Final gas pressure	32.3 GPa	32.3 GPa	13.8 GPa	13.8 GPa
Final gas density	2,145 kg/m^3	2,145 kg/m^3	1,590 kg/m^3	1,590 kg/m^3
Final gas temperature	5,274 K	5,274 K	3,710 K	3,710 K
Final gas velocity	3,029 m/s	3,029 m/s	1,291 m/s	1,291 m/s
(Final gas Mach number)^2	0.567	0.567	1.99	1.99
Maximum gas temperature	12,526 K	12,524 K	3,710 K	3,710 K
Final solid pressure	0.745 GPa	0.810 GPa	.657 GPa	.771 GPa
Final solid density	1,976 kg/m^3	1,987 kg/m^3	1,967 kg/m^3	1,982 kg/m^3
Final solid temperature	351 K	354 K	345 K	352 K
Final solid velocity	306 m/s	134 m/s	273 m/s	119 m/s
(Final solid Mach number)^2	5.63	5.82	5.78	5.89

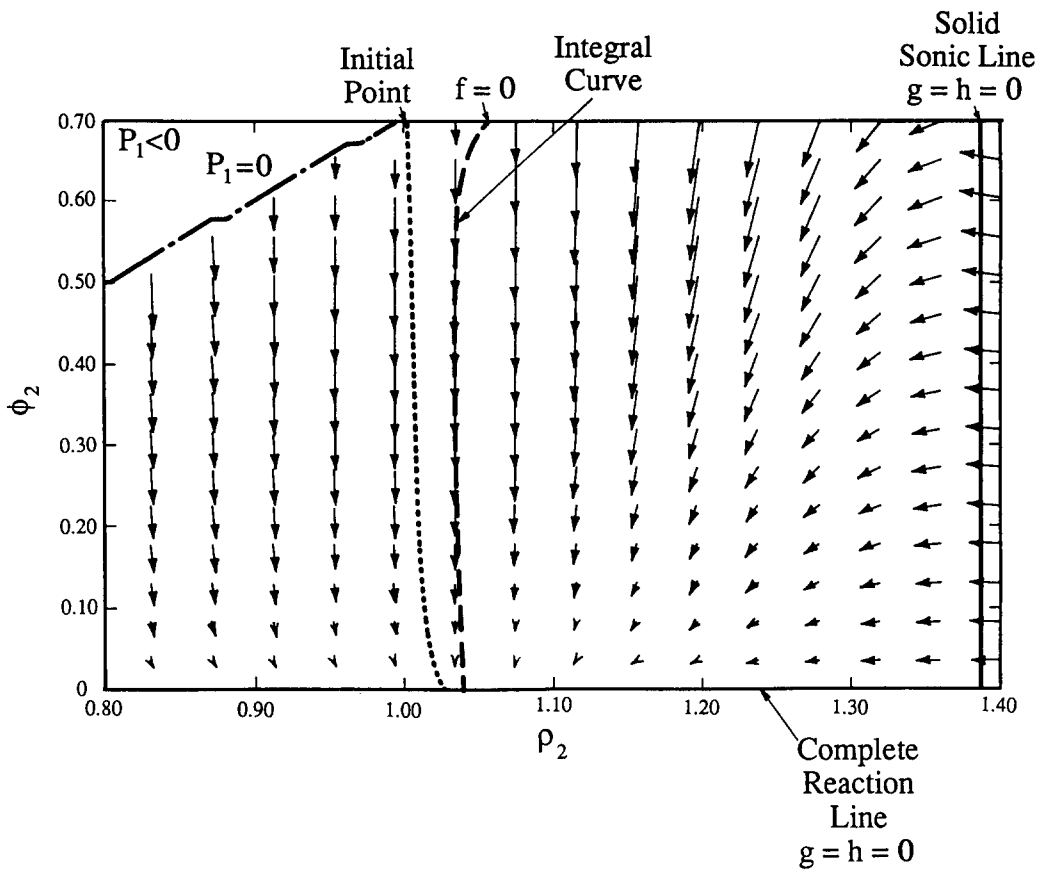

Fig. 9. Phase plane for strong detonation, $D > D_{CJ}$.

show results of more complicated one-phase models that indicate that a unique weak wave speed exists when such mechanisms as diffusive heat and momentum transfer are taken into account. A similar result may hold for two-phase detonations.

DISCUSSION AND CONCLUSIONS

The most important result of this study is that existence conditions have been predicted for a steady, one-dimensional, two-phase detonation in a granular material. The available detonation solutions are restricted by both algebraic equilibrium end state analysis and by an analysis of the structure of the steady wave. The structure analysis has shown that for a structure with a single lead gas shock and an unshocked solid, below a critical initial bulk density no steady solution can exist. This particular result and the general technique of using structure analysis to limit the available solutions is new to two-phase detonation theory.

As a result of this study it is possible to predict the features of a steady two-phase detonation structure. It has been shown that two-phase equivalents to the one-phase ZND strong and CJ solutions can be predicted. As in one-phase ZND theory, the two-phase theory predicts that piston support is required for the strong solution to exist, and that a two-phase CJ detonation can propagate with or without piston support. It has also been shown that when both the gas and solid phases are unshocked, the model equations yield two-phase equivalents of weak and CJ solutions. These types of solutions are also found using the simple one-phase ZND theory but are commonly dismissed because it is thought that there is no mechanism

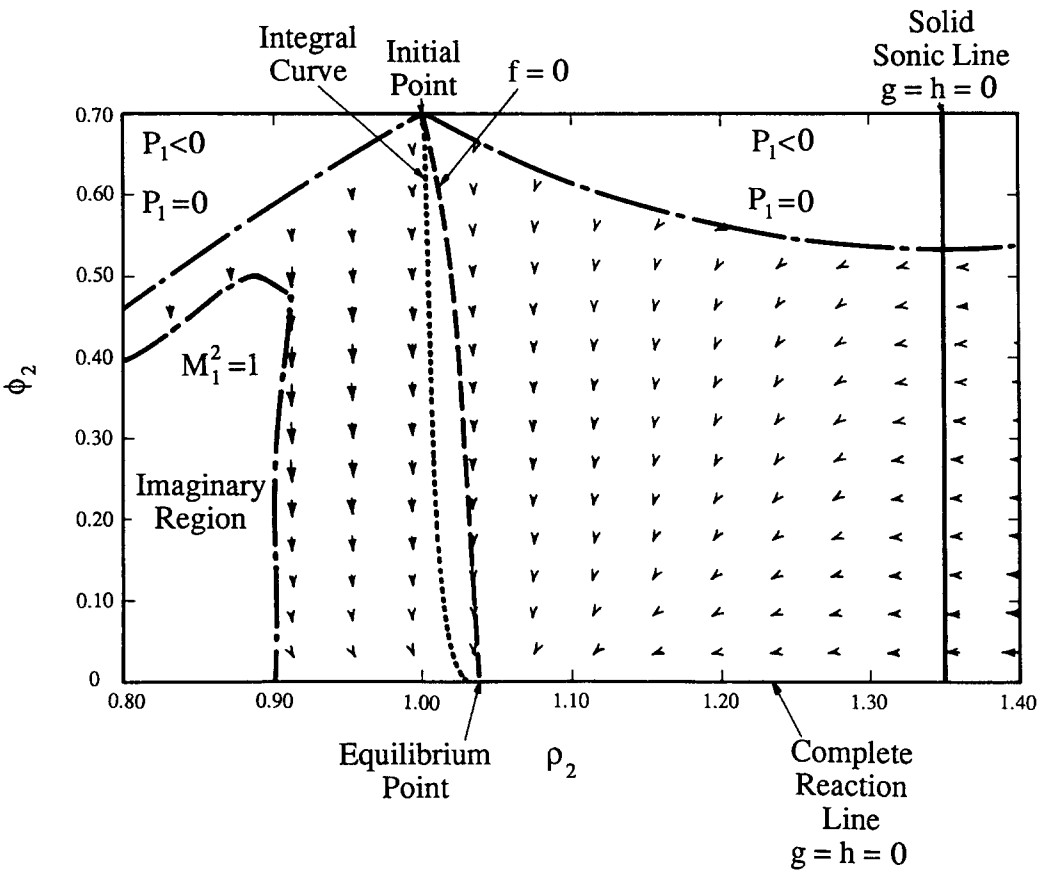

Fig. 10. Phase plane for weak detonation, $D > D_{CJ}$.

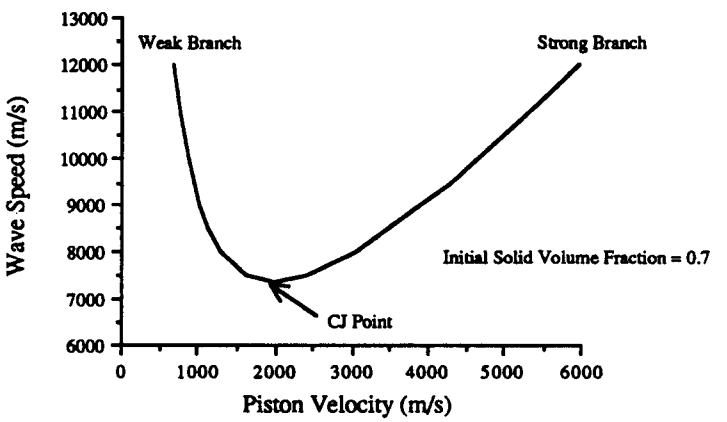

Fig. 11. Two-phase detonation wave speed vs. piston velocity.

to initiate reaction. The model yields such solutions because the functional form of the combustion model allows a small amount of reaction to occur even at ambient conditions.

Some results plotted in Fig. 3 and listed in Tables 2 and 3 may be viewed by some as unrealistic. For instance the differences in gas and solid pressures and temperatures in the reaction zone could be seen as large, especially when one considers common phenomena, which do not occur in the extreme conditions of a detonation. Viewed in another way these results could be plausible. The results are primarily the consequence of certain modeling assumptions and parameter choices. These choices were made to a large extent to ensure that a steady detonation structure could be predicted. As stated earlier, a primary objective of this article is to highlight the technique of two-phase steady modeling and to place two-phase detonation theory in the context of one-phase detonation theory. As such, parameters were chosen with more freedom than in a study designed to precisely predict physical variables.

Despite this uncertainty, the results here do have value and may be as accurate as any other prediction. There are not good experimental ways to determine the details of the detonation reaction zone structure. As such, the functional forms of the phase interaction terms and state equations are uncertain in all models. One reasonable expectation of a two-phase model is that it be able to match predictions of the equilibrium TIGER code, which this model is able to do well.

Although not considered in this study, one may ask how the scenario of a shocked gas and unshocked solid could develop. To speculate, one could imagine a slow, unconfined burning of reactive particles. If the system were suddenly confined, a local region of high gas pressure could develop, giving rise to a propagating shock wave in the gas but not the solid. It should also be noted that the idea of shocked gas and unshocked solid is common in the literature of shock waves in dusty gases. A standard assumption is that there is a shock wave in the gas but that the solid particles are incompressible, thus unshocked. Rudinger [22] provides an example of such a model.

Much work remains to be done in two-phase detonation theory. It is highly likely that other classes of steady detonations can be predicted. The complexity of the model equations makes this search largely a trial and error process. However, one can envision several different detonation scenarios by making minor adjustments in the relative positions of the separatrices in the two-dimensional phase plane.

Two-phase steady detonation results can be effectively used in the unsteady two-phase DDT problem. Predictions of any unsteady model would be strengthened by comparing them to the predictions of a steady model. Unsteady model results can be used to verify that the unsupported two-phase detonation wave is a CJ wave. This would simply require an examination of the two-phase end state conditions.

Reaction zone lengths predicted by the steady model must match those predicted by the unsteady model. This, however, raises an important question regarding numerical resolution. This study predicts reaction zone lengths of the order of 10 mm. Unsteady two-phase models now use a cell size on the order of 1 mm. Thus the results of this study suggest that a cell size on the order of 0.01–0.1 mm be employed in unsteady calculations.

Cell sizes of this magnitude present a dilemma. Typical particle sizes for detonation applications range from 0.1 to 1 mm. One assumption of continuum modeling of granular materials is that a large number of particles exist in any averaging volume. If cell sizes of the order of 0.01–0.1 mm are employed, as the results suggest is necessary, then the continuum assumptions may not be valid.

REFERENCES

1. Griffiths, N., and Groocock, J. M., *J. Chem. Soc. Lond.* 814:4154–4162 (1960).
2. Bernecker, R. R., and Price, D., *Combust. Flame* 22:111–118, (1974).
3. Bernecker, R. R., and Price, D., *Combust. Flame* 22:119–129 (1974).
4. Butler, P. B., Lembeck, M. F., and Krier, H., *Combust. Flame* 46:75–93 (1982).
5. Butler, P. B., Krier, H., *Combust. Flame* 63:31–48 (1986).
6. Baer, M. R., and Nunziato, J. W., *Int. J. Multiphase Flow* 12:861–889 (1986).

7. Baer, M. R., Gross, R. J., Nunziato, J. W., and Igel, E. A., *Combust Flame* 65:15-30 (1986).
8. Akhatov, I. Sh., and Vainshtein, P. B., *Combust. Explos. Shock Waves* 20:63-69 (1984).
9. Markatos, N. C., *Int. J. Multiphase Flow* 12:913-933 (1986).
10. Krier, H., and Mozaffarian, A., *Int. J. Multiphase Flow* 4:65-79 (1978).
11. Powers, J. M., *Theory of Detonation Structure for Two-Phase Materials*, Ph.D. thesis, University of Illinois at Urbana-Champaign, 1988.
12. Sharon, A., and Bankoff, A., *Int. J. Heat Mass Transf.* 24:1561-1572 (1981).
13. Condiff, D. W., *Int. J. Heat Mass Transf.* 25:87-98 (1981).
14. Fickett, W., and Davis, W. C., *Detonation*, University of California Press, Berkeley, 1979, p. 13.
15. Powers, J. M., Stewart, D. S., and Krier, H., *Prog. Astronaut. Aeronaut.* 114:341-361 (1988).
16. Powers, J. M., Stewart, D. S., and Krier, H. *Combust. Flame* 80:264-279.
17. Baer, M. R., and Nunziato, J. W., Sandia National Laboratories Technical Report SAND 82-0293, 1983.
18. Coperthwaite, M., and Zwisler, W. H., Stanford Research Institute Report PYV-1281 (1974).
19. Marsh, S. P., Ed., *LASL Shock Hugoniot Data*, University of California Press, Berkeley, 1980, p. 596.
20. Sandusky, H. W., and Bernecker, R. R. in *Proceedings of the Eighth Symposium (International) on Detonation*, NSWC MP 86-194, Naval Surface Weapons Center, White Oak, MD, 1985, p. 881.
21. Powers, J. M., Stewart, D. S., and Krier, H., *J. Appl. Mech.* 56:15-24 (1989).
22. Rudinger, G., *Phys. Fluids* 7:658-663 (1964).

Received 23 September 1988; revised 30 June 1989